IJAMMP

Deformation Behaviour in the New Backward Extrusion Process of Pure Copper through Different Die Geometries

Moein Shahveh, Ghader Faraji*

RESEARCH ARTICLE

ARTICLE INFO

Keywords:

New backward extrusion;
Finite Element analysis;
Severe plastic deformation;
Optimization process.

Article History

*Received:*24 October 2025
*Revised:*19 February 2026
*Accepted:*28 February 2026
Published:

ABSTRACT

This study investigated the effects of die geometry on the required forces and strains in the new backward extrusion (NBE) process. The force requirements for copper extrusion were determined using the finite element method, and the relationships between die geometry and process parameters on extrusion force and plastic strain were examined. The process efficiency was evaluated under various working conditions by examining the relationship between geometric variables and speed. This innovative approach, which uses hydrostatic pressure techniques, shows potential to transform billets into ultrafine-grained tubes and materials that are difficult to deform. The results indicate that modifications to the fix-punch geometry significantly reduce the required extrusion force. In all cases, the extrusion force initially increased as the billet entered the deformation zone, then decreased as material continued to flow. Maximum extrusion loads of 109 kN and 91.8 kN were obtained for fix-punch designs with inner channel angles of 30° and 45°, respectively. In comparison, a lower maximum load of 94.2 kN was observed for the geometry with an inner channel radius of 12.5 mm. The FEM results further revealed that the equivalent plastic strain (PEEQ) was strongly dependent on fix-punch geometry, with maximum PEEQ values ranging from approximately 2 to 2.5, primarily concentrated near the die corner and along the radial deformation path. Compared with angled channel designs, the radial geometry resulted in reduced force demand and a more gradual strain distribution during the NBE process.

1. Introduction

In recent years, significant research efforts have been directed toward the development of novel manufacturing processes for high-performance materials in advanced applications (H. Rahimi et. al, 2025). Obtaining fine-grained materials with excellent mechanical characteristics is very important (Mao et. al., 2021). Severe plastic deformation (SPD) techniques have garnered substantial interest as efficient methods for generating bulk ultrafine-grained (UFG) and nanostructured metals and alloys while maintaining overall dimensions (Taherkhani et al., 2025). Materials processed by SPD generally exhibit significantly elevated strength, extended fatigue life, superior formability or superplasticity, and, in many cases, greater wear and corrosion resistance, rendering them highly desirable for industrial applications (Ahmadi, et al. 2021; Faraji, et al., 2018). Tubes are of particular importance, especially among the diverse product geometries for applications in heat exchangers, energy systems, and lightweight structures,which has led to the Development of SPD forming techniques (Lowe & Valiev, 2000; Valiev et al., 2016; Zohrevand et al., 2023).

Department of Mechanical Engineering, College of Engineering, University of Tehran, Tehran, 11155-4563, Iran

*Corresponding author : ghfaraji@ut.ac.ir

Several processes have been proposed for producing thin-walled tubular components with large imposed strains, including Parallel Tubular Channel Angular Pressing (PTCAP) (Awasthi et al, 2022), Tube Backward Extrusion (TBE) (Abu-Farha, 2012), High Pressure Tube Twisting (HPTT) (Toth et al., 2019), Friction Stir Back Extrusion (FSBE) (El Mehtedi et al., 2019), and Tube High Pressure Shearing (t-HPS) (Wang et al., 2012).

However, many reported configurations remain limited by disadvantages such as high forming forces, non-uniform strain distribution, complex tools, and limited scalability for long tubes or closed geometries. Consequently, Optimization of existing processes and development of modified mold concepts, especially for industry-relevant alloys and tubular products, remain active research topics to reduce energy consumption and improve strain homogeneity (Faraji et al. 2011; Jafarlou et al., 2016; Majidabad et al., 2023).

To address some of the limitations of SPD Processes for tube production, severl studies have been conducted. Motallebi et al., (2021) showed that applying hydrostatic force in Hydrostatic Tube Cyclic Expansion Extrusion (HTCEE) significantly improves material flow and reduces the required forming load, while creating a more uniform strain distribution. Bakhshi-Jooybari et al. (2006), focused

on reducing deformation load in BE by optimizing the die profile using numerical simulation and experimental methods. Shatermashhadi et al.,(2014) presented the NBE instead of conventional backward extrusion to reduce the force required for backward extrusion and increase plastic strain by including a fix-punch section. Adding this section results in a decrease of more than 25% in the force required for production compared to the standard backward extrusion process. Manaafi et al., (2016) have presented techniques to enhance the NBE process, including the use of hydrostatic force, resulting in an 11% reduction in the process power requirement.

The NBE produces ultrafine-grained metals characterized by enhanced mechanical strength and optimized microstructural properties. This method is suitable for closed-end products and offers benefits compared to alternative production methods. Some benefits of this method include reduced material usage, increased dimensional accuracy and surface quality, appropriate mechanical and microstructural properties, and reduced additional steps. To reduce the force and energy required in the SPD process, the optimization of this group of forming processes has received much attention. Failure to consider die design parameters when studying metal deformation can result in excessive energy requirements and inaccurate results, despite efforts to achieve the best possible outcome.

FEM is an important approach for understanding the plastic deformation behavior of materials in forming processes (Dixit & Dixit, 2008). Numerical analysis using FEM was performed to evaluate material deformation and predict strain and stress distributions. The plastic deformation behaviour during the BE process is mainly controlled by the die geometry, the material, and the process conditions (Zeng et al., 2024). Despite numerical and experimental investigations on NBE, the specific influence of the internal channel geometry of the fix-punch on the force, strain distribution and strain homogeneity in the NBE process has not been systematically determined. In particular, comparative analyses between angle channels and radius geometries under the same processing conditions are still limited. Therefore, this study investigates the plastic deformation characteristics of commercial pure copper in NBE, as assessed by finite element analysis, variations in extrusion force, and strain progression. Previous research has shown that changing the die geometry can increase the applied equivalent strain and facilitate the development of fine-grained and granular structures. This study systematically analyzes the effects of different die geometries on the effective strain distribution and extrusion force requirements in the NBE process of copper, with the aim of establishing design guidelines to optimize die geometry for energy efficiency, strain uniformity in thin-walled and closed-end products.

2. Methodology

Finite element simulations of the NBE process were performed using Abaqus/Explicit 2021 to investigate the effect of die geometry on deformation behavior, extrusion force, and strain distribution. An axisymmetric model that matched the geometry and mechanical properties of the experimental samples was developed to validate FEM results against experimental data. In the next step, boundary conditions were defined to prevent rigid-body motion of the billet while allowing free material flow within the deformation channel. Reaction forces on the movable punch were recorded to evaluate the evolution of the extrusion load throughout the process. CAX4R elements were used to represent the axisymmetric billet, with mesh sizes ranging from 0.05 to 1.4 mm. Adaptive Lagrangian-Eulerian elements (ALE) were specifically designed and tuned to handle significant deformations and are utilized in simulations. Thus, using ALE techniques improved mesh quality during simulation of SPD processes. The workpiece exhibited a friction coefficient of 0.05 when in contact with the die components. Additionally, a friction coefficient (μ) of 0.05 was considered for the billet's contact with other deformed sections during the process.

During the NBE, the movable punch descended while other die components remained stationary. Fig. 1 shows the starting and ending points of the movable punch during the process, along with the material flow direction in various ways. The punching velocity was set to 10 mm/min. To investigate the effect of die geometry on the NBE process, three fix-punch configurations were analyzed, including inner channel angles of 30° and 45°, and an inner channel radius of 12.5 mm. The selected geometric parameters were chosen to represent sharp, intermediate, and smooth material transfer conditions commonly encountered in extrusion die design. The inner channel angle of 30° was considered to impose higher material flow resistance due to the abrupt change in flow direction, whereas the inner channel angle of 45° provided a smoother material transition with reduced geometric constraint. The use of the inner channel radius of 12.5 mm was intended to minimize stress concentration at the die corner and to promote a more gradual and uniform material flow during the NBE process. Other geometric parameters, including billet dimensions, channel length, and final tube thickness, were kept constant to ensure a consistent comparative analysis. Pure copper was the material utilized in the simulation. Since the die remained elastic and underwent negligible deformation, it was modeled as a rigid body (Uyyuru & Valberg, 2006). Table 1 lists the density, Young's modulus (E), Poisson's ratio (ν), yield strength, and ultimate strength of copper. Fig 2 displays the stress-strain curve for pure annealed copper.

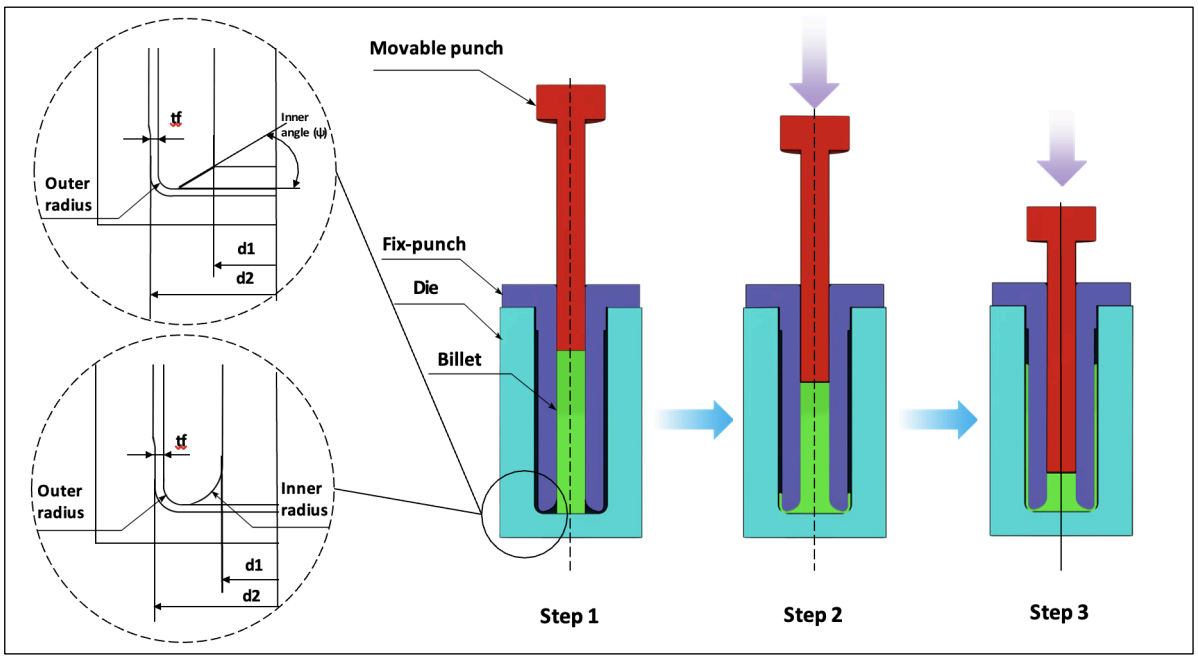

Figure 1. Schematic illustration of the NBE process

Table 1. Mechanical properties of pure copper

Simulation Parameters	Values
Density (kg.m^{-3})	8900
Modulus of Elasticity (GPa)	110
Tensile Strength, Yield (MPa)	33.3
Elongation at Break (%)	60
Poisson's ratio	0.34
Stress-relief annealing temperature (°C)	250-500

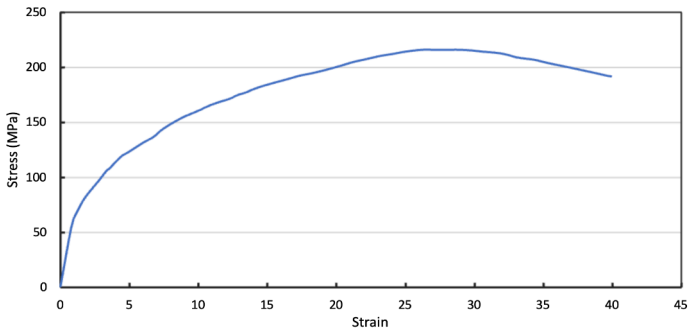

Figure 2. Stress-strain curve of pure copper used in FE modeling

This process involves creating the product from a copper billet that has an initial length of 150 mm and a diameter of 25 mm. Table 1 contains the initial billet parameters. Fig. 1 shows the geometric parameters that have been modified throughout the analysis procedure, with the inner diameters (d1) and outer diameters (d2) and final thickness (tf) remaining constant. FEM simulations were conducted to study deformation patterns and material properties by varying the inner channel angles, the inner channel radius, and the channel shape.

Fixed values are used for additional parameters such as the initial billet diameter, movable punch diameter, and billet height. Initially, the tube is stretched outward through a passage at the inner channel angles of ψ = 45°, 30°, and with the inner channel radius of r1 = 12.5mm, after which the billet thickness is decreased to tf. In the end, the narrow tube with a diameter (d2) inside is flipped through the second channel. Extrusion through angled channels and thickness reduction in the NBE process result in significant deformation of the tube material, producing a thin-walled tube with ultra-fine grain structure. The main factors for analysis are the gap height, channel height, and die shape. Table 2 lists the parameters examined and evaluated in the design. It is important to note that this statement requires experimental evidence.

Table 2. Process parameters and simulation conditions for NBE

Simulation Type	axisymmetric
Die Type	Rigid Body
Billet Type	Deformable
Billet material	Cu
Press speed (mm/min)	10
Billet temperature (°C)	25
Channel length (mm)	180
Channel diameter (mm)	2
Height of billet (mm)	150
Diameter of billet (mm)	25

3. Results and Discussion

FEM simulation results for movable punch load, stress, and applied strains were significant, and the development of Equivalent Plastic Strain (PEEQ) and force at various stages of NBE processing are shown in Figs. 3, 4, and 5.

Fig. 3 shows the movable punch load-displacement behavior for three fix-punch geometries with the inner channel angles of 30° and 45°, and the inner channel radius of 12.5 mm. The maximum movable punch load was evaluated for each geometry. A constant channel height and a friction coefficient of μ=0.05 were maintained throughout the simulations. The load-displacement curves provided valuable insight into the deformation mechanics and force requirements of the manufacturing process. In Zone I, the load increased rapidly as the billet head entered the deformation channel. This stage occurs when the billet head enters the channel. The force difference in this stage was slight. However, the force required in the channel is initially low and increases as material flows through. With the inner channel radius of 12.5 mm, the force remained lower than that of the other geometries at this stage. Zone II represented a transition stage marked by an initial minor load increase, followed by a prominent force surge as the material reached the narrower confined channel section. In the second stage, the load dropped from its peak to a local minimum, followed by a slight increase in Zone III. The cases examined with the inner channel radius of 12.5 mm and the inner channel angle of 45° show that at the onset of Zone III, the billet struck the channel wall. Until the billet was entirely inside the channel, a slight increase in force was observed

A prominent force surge was detected in Zone V for the inner channel angle of 30°, signifying substantial changes in billet shape. Notably, the inner channel angle of 30° requires significantly higher force during this stage than other geometries, leading to less stable material flow and increased load volatility. The peak movable punch load for the inner channel angle of 30° reached approximately 109 kN, and using the inner channel radius of 12.5 mm resulted in approximately an 18% reduction in applied force relative to the inner channel angle of 30°, yielding notable cost and energy savings.

Fig. 4 shows the material flow for each fix-punch geometry at the successive stages of the NBE process. Specifically, Figs. 4(a–d) show the complete deformation geometry and billet configuration for a channel with the inner channel angle of 30°, Figs. 4(e–h) show the corresponding geometry for a channel with an inner angle of 45°, and Figs. 4(i–l) shows the deformation sequence for a channel with the inner channel radius of 12.5 mm. In all three geometries, material continuously fills the channel during all deformation stages. This uninterrupted contact between the material and channel surface is maintained by back pressure, which prevents material separation and ensures continuous deformation. The continuous filling behavior observed across all scenarios underscores the critical role of back pressure in maintaining the integrity of the material flow during extrusion. The deformation patterns observed in all geometries indicate a steady progression of material towards the channel exit. This consistency indicates a steady and uniform flow of material through the channel. Such uniformity is essential to achieve consistent

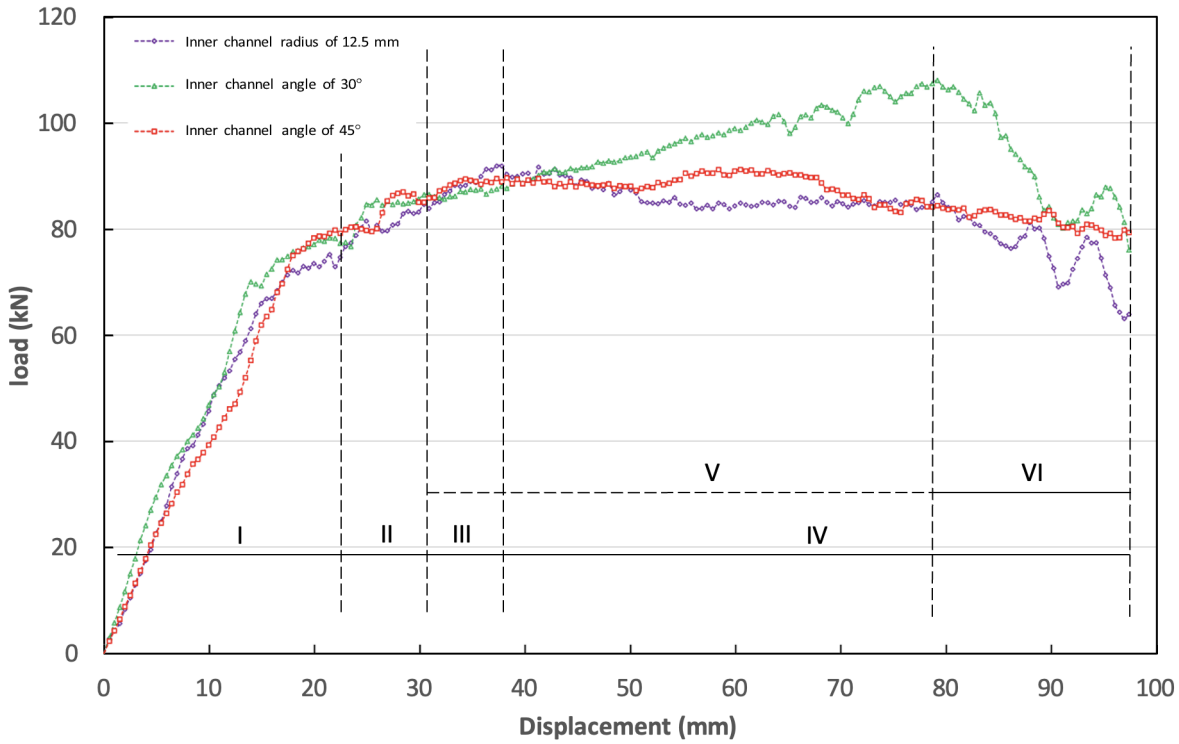

Figure 3. Load-displacement behavior in fix-punch geometries with the inner channel angles of 30°, 45°, and the inner channel radius of 12.5 mm.

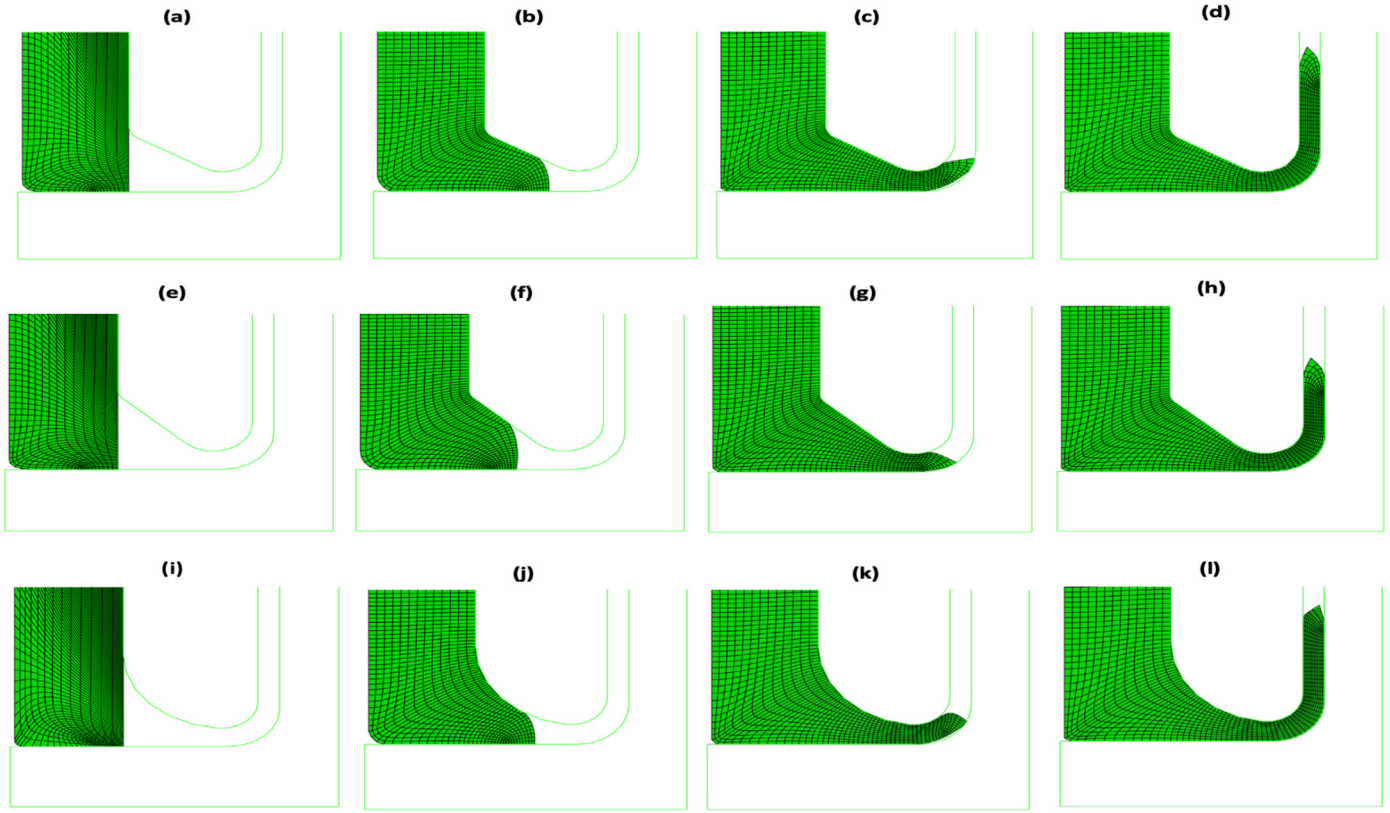

Figure 4. Investigating FEM material flow according to the change of fix-punch geometry parameters with (a-d) channel with the inner channel angle of 30°, (e-h) channel with the inner channel angle of 45°, and (i-l) channel with the inner channel radius of 12.5 mm

microstructural features and mechanical properties in the extruded product. The results show that within the range of geometries studied, the backpressure mechanism effectively controls the material distribution and prevents flow instabilities that may compromise product quality.

Fig. 5 shows the PEEQ distribution in closed-end copper tubes processed with three distinct fix-punch geometries. The results show significant accumulation of PEEQ in the corner and die-entry regions, where the material undergoes the most severe deformation. The strain distribution is highly non-uniform across all examined geometries, with the maximum strains concentrated in regions of highest geometric constraint. The inner channel angle of 30° shows the highest strain in the corner region, while the inner channel angle of 45° and inner channel radius of 12.5 mm show similar, but intensity-dependent, patterns. The variation in strain distribution in these geometries indicates the influence of the die angle and corner radius on the material deformation paths. An important observation is that the spatial distribution and magnitude of strain vary significantly with fix-punch geometry and the progression of the extrusion process. The material in the movable punch region experiences minimal strain, while the material adjacent to the die corner undergoes severe plastic deformation. This inhomogeneous strain field indicates that the die geometry directly controls the intensity of local deformation and the material flow paths. Geometries with larger corner radius or more acute angles produce more gradual material deformation, thereby reducing local strain concentration. The non-uniform strain distribution underscores the need to carefully optimize the die design to achieve balanced material deformation and minimize mechanical property degradation in the extruded product.

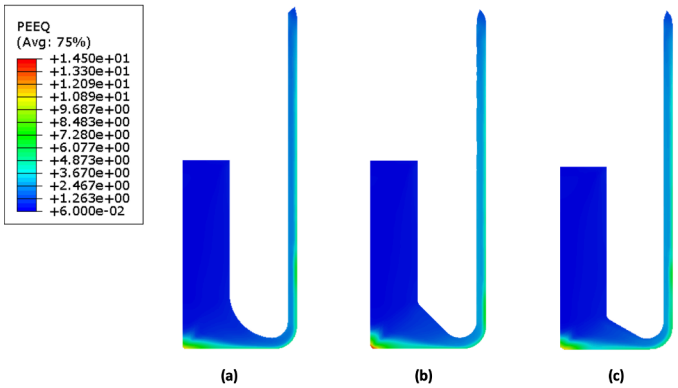

Figure 5. distribution of PEEQ in closed-end copper tubes processed by NBE with varying fix-punch geometries: (a) inner channel radius of 12.5 mm, (b) inner channel angle of 45°, and (c) inner channel angle of 30°.

Some SPD processes, which operate either entirely or partially under pure shear conditions, are derived from conventional metal-forming techniques such as rolling, extrusion, and forging. These procedures involve repeated deformation cycles that generate inhomogeneous strain distributions, resulting in non-uniform microstructure and mechanical properties (Faraji et al., 2024; F. Rahimi et al., 2015). Consistent with this, the non-uniform distribution of

PEEQ in the cross-section of the tube after backward extrusion was observed, as shown in Fig. 5. The PEEQ distribution in the extruded tube was evaluated along two measurement paths. The longitudinal path AD, which extends from the tube inlet (point A) to the closed end (point D), and the radial path EF, which passes through the wall thickness from the inner surface (point E) to the outer surface (point F). Fig. 6 shows the PEEQ profiles for each die geometry investigated.

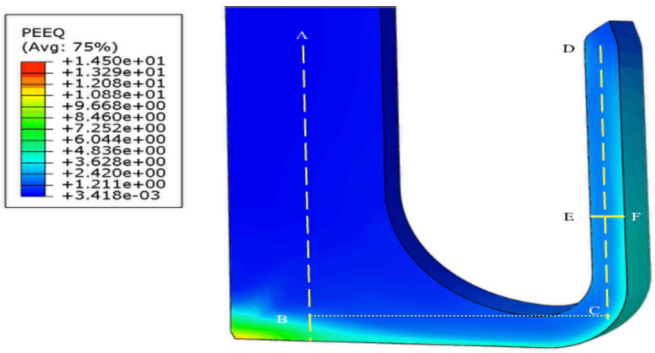

Figure 6. Measurement paths for PEEQ analysis showing radial (EF) and longitudinal (AD) directions on the extruded closed-end tube cross-section

Fig. 7 shows the radial distribution of PEEQ across the tube thickness, examining three distinct die geometries processed via conventional reverse extrusion. The EF measurement path shown in Fig. 6 extends radially from the inner surface of the tube to the outer surface. The strain profiles show a consistent pattern across all geometries. The PEEQ values remain relatively stable in the inner regions, but increase significantly as the material approaches the outer surface. The closed-end tube produced with the inner channel angle of 45° exhibits superior strain uniformity across the wall thickness. The strain variation between inner and outer surfaces is minimal, indicating more consistent properties throughout the wall thickness. The inner channel angle of 30° shows inner PEEQ values averaging 2.69 and outer values reaching 5.76, representing a radial strain increase of approximately 115%.

The inner channel angle of 45° exhibits an internal strain of 2.76 and an external strain of 4.79, corresponding to a radial increase of 74%. The inner channel radius of 12.5 mm exhibits the most pronounced gradient, with inner surface strain of 2.29 and outer surface strain of 6.25, representing a radial increase of 173%. These differential gradients reflect the distinct flow characteristics imposed by each die geometry.

The maximum external surface strain resulting from the inner channel radius of 12.5 mm is 8.6% greater than the inner channel angle of 30° and 28.5% greater than the inner channel angle of 45°. The high plastic deformation on the outer surface promotes progressive grain refinement,

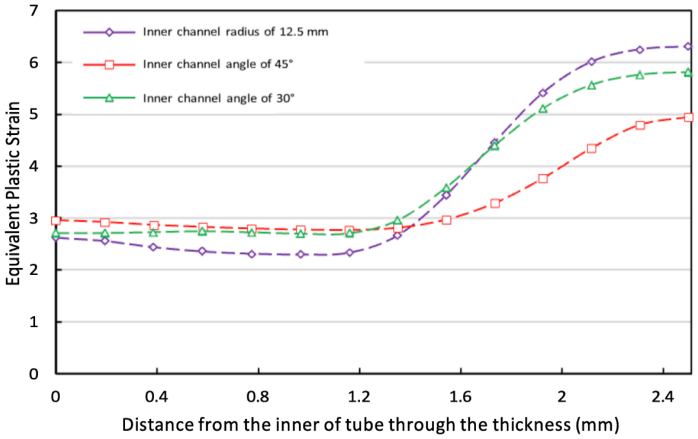

Figure 7. The radial distribution of PEEQ indicates the strain evolution from the inner to the outer surfaces (path EF) of the tube for the three fix-punch geometries examined.

potentially providing superior surface mechanical properties for applications requiring high wear and fatigue resistance (Taherkhani et al., 2024; Taherkhani et al., 2025).

In contrast, the inner channel angle of 45° exhibits better strain uniformity throughout the tube wall thickness. The strain difference between the inner surface (2.76) and outer surface (4.79) is 2.03, representing a 74% radial increase and indicating more uniform property distribution across the cross-section. This differential uniformity reflects an opposing design philosophy. While the inner channel radius of 12.5 mm concentrates deformation toward the outer surface, the inner channel angle of 45° distributes strain more evenly, improving uniformity of the microstructure throughout the tube thickness. In the Accumulative Back Extrusion (ABE) process, a plastic strain of ~4 can be obtained. Higher plastic strain in the inner channel radius of 12.5 mm correlates with a finer grain size and improved mechanical properties (Li et al., 2014). Therefore, the inner channel radius of 12.5 mm offers significant advantages for producing ultrafine-grained copper tubes.

In the direction of AD (shown in Fig. 6), the primary billet underwent significant deformation along the final product due to the strong force from the movable punch. The longitudinal strain distribution along the tube length exhibited distinct deformation characteristics that vary significantly with the die geometry. Fig. 8 shows the evolution of the effective strain in four consecutive zones during a typical reverse extrusion process. In Zone I, the material entered the deformation zone with minimal initial strain (~0.2). However, upon contact with the die geometry, it experienced rapid strain accumulation, with peak values reaching approximately 2.8–3.0 in all geometries. This zone represented the transition from the fix-punch channel entry to the confined channel section. Zone II constituted a transition zone in which strain values stabilized and begin to diverge across the three geometries, and the material gradually fills the channel. Zone III showed stable strain differentiation, with the inner channel angle of 30°

exhibiting significantly higher strain intensity than both the inner channel angle of 45° and the inner channel radius of 12.5 mm geometries, reflecting the stronger geometric constraints of acute angles.

Zone IV, representing the channel exit region, showed stable, convergent strain values of approximately 2.0–2.5 across all geometries, indicating progressive strain homogenization as the material approached the extrusion exit and geometric constraints were reduced. Once the material is fully introduced into the final channel (Zone IV), the effective strain becomes relatively uniform, with less than 10% variation along the channel length across all three geometries. The final PEEQ ranged from 2 to 2.5, indicating significant cumulative deformation. In contrast, achieving comparable strains with equal-channel angular pressing (ECAP) requires multiple passes. Therefore, NBE demonstrated superior efficiency in generating high cumulative plastic strain in a single pass.

Analysis of the simulation results has shown that significant strain inhomogeneities are generated throughout the final product. Die geometry, fix-punch design, and friction conditions affect material flow patterns. The purpose of the strain inhomogeneity index (Ci) is to verify the uniformity of the effective strain distribution within the sample's cross-section (Lee & Kim, 2014). Enhancing uniformity in deformation results in greater consistency in the mechanical characteristics of UFG materials. Specifically, the level of the strain inhomogeneity can be assessed by Eq. 1:

Fig. 9 shows the strain heterogeneity along the tube thickness. The inner channel angle of 45° has the lowest heterogeneity index of 0.60, indicating a relatively uniform and suitable strain distribution. The inner channel angle of 30° produces a higher index of 0.82, while the inner channel radius of 12.5 mm produces the highest heterogeneity of 1.09. These results indicate that the inner channel angle of 45° produces approximately 45% improvement in strain uniformity compared to the inner channel radius of 12.5 mm. The quantitative evaluation presented in Fig. 10 shows that the inner channel angle of 30° has the highest longitudinal strain heterogeneity index of 1.61, confirming that this geometry imparts significant strain variations in the final product. The inner channel angle of 45° yields an average value of 1.56.

In contrast, the inner channel radius of 12.5 mm yielded the lowest strain heterogeneity index of 1.52, indicating the most uniform strain distribution in the direction of material flow in the extrusion. This superior longitudinal uniformity in the inner channel radius of 12.5 mm resulted from the smooth, gradual transition provided by the curved geometry, which progressively loaded the material rather than creating sharp geometric discontinuities. This uniformity in longitudinal strain indicated more stable material flow throughout the deformation region. These findings emphasized that the geometric design significantly influenced the plastic strain distribution, with potential implications for microstructural development and property uniformity in the final extruded product.

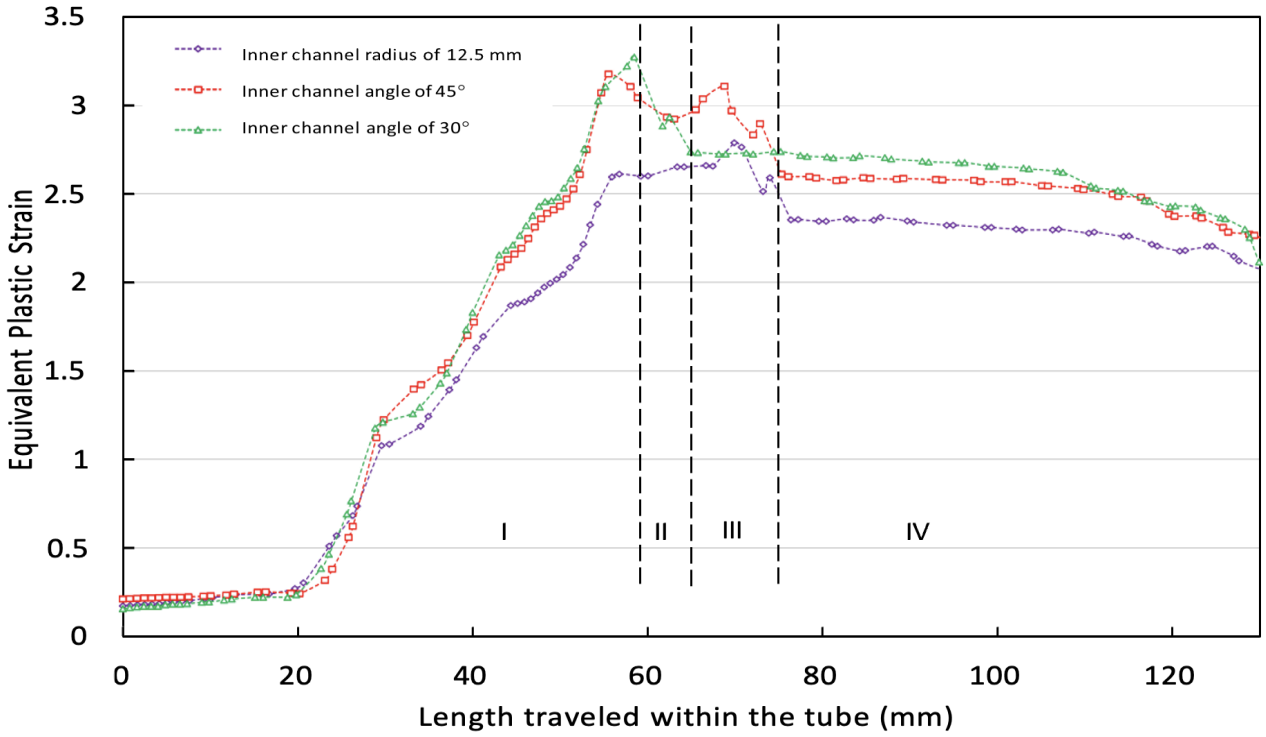

Figure 8. PEEQ distribution along the length of the tube (path AD) for three fix-punch geometries.

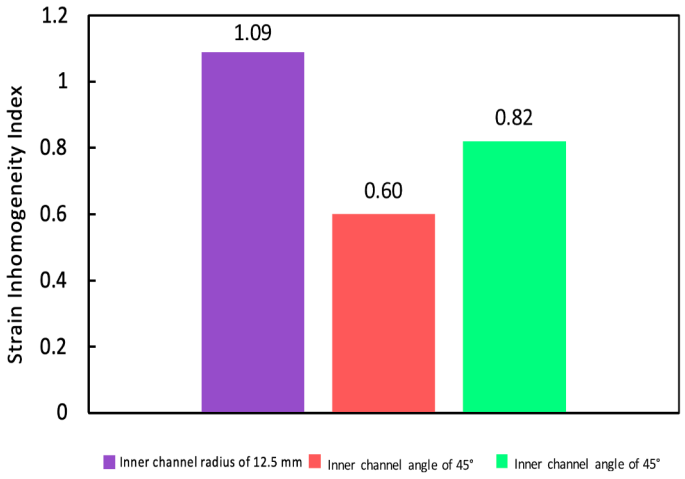

Figure 9. Radial distribution of the strain inhomogeneity index throughout the tube thickness for inner channel angles of 45°, 30°, and an inner channel radius of 12.5 mm.

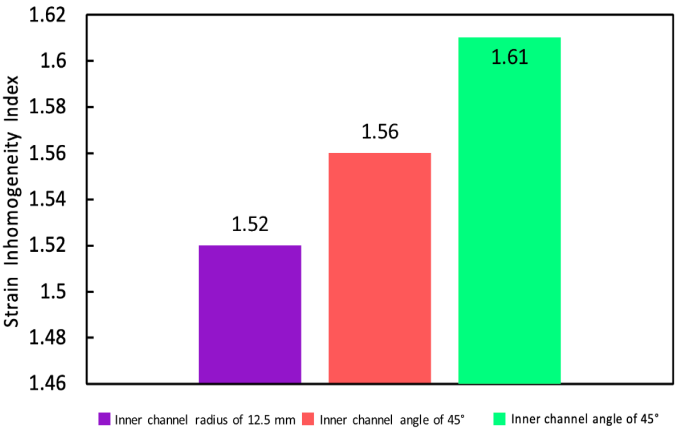

Figure 10. Evolution of the strain inhomogeneity index along the tube length for inner channel angles of 45°, 30°, and an inner channel radius of 12.5 mm

4. Conclusions

This FEM analysis showed that precise die geometry optimization in NBE provides a powerful means to control plastic strain distribution, reduce process forces, and improve the quality of the final product. The quantitative relationships established between the die geometric parameters and final product properties provide a rational framework for die designs. The conclusions are as follows:

- FEM findings indicated that plastic strain exceeding 3.5 was observed in all three cases examined.
- The inner channel angle of 45° resulted in an 18% decrease in required force compared to the inner channel angle of 30°. Hence, reducing the pressure can potentially lead to reduced press capacity and increased die life.
- The die geometry optimization addresses movable punch buckling issues that arise during processing. Additionally, it facilitates extrusion of small-diameter billets that are difficult to form with conventional geometries.
- The uniformity of plastic deformation across the tube width after processing was significantly better than in other instances using a channel with the inner channel radius of 12.5 mm.
- Once the material fills the final channel in the NBE process, it leads to a uniform distribution of plastic deformation and a significant reduction in strain variations along the tube, playing a key role in achieving stable material flow, promoting strain homogeneity, and improving the quality of the final product.

In future research, it is necessary to focus on experimental validation of FEM results to confirm the predicted parameters, particularly the force and strain distributions. Also, developing analyses and establishing relationships between strain homogeneity and microstructural features can provide a more comprehensive understanding of the impact of die geometry on final product performance.

References

Abu-Farha, F. (2012). A preliminary study on the feasibility of friction stir back extrusion. *Scripta Materialia, 66*(9), 615-618.

Ahmadi, S., Faraji, G., Alimirzaloo, V., & Donyavi, A. (2021). Microstructure and mechanical properties of AM60 magnesium alloy processed by a new severe plastic deformation technique. *Metals and Materials International, 27*(8), 2957-2967.

Awasthi, A., Rao, U. S., Saxena, K. K., & Dwivedi, R. K. (2022). Impact of equal channel angular pressing on aluminium alloys: An overview. *Materials Today: Proceedings, 57*, 908-912.

Bakhshi-Jooybari, M., Saboori, M., Hosseinipour, S., Shakeri, M., & Gorji, A. (2006). Experimental and numerical study of optimum die profile in backward rod extrusion. *Journal of Materials Processing Technology, 177*(1-3), 596-599.

Basavaraj, V. P., Chakkingal, U., & Kumar, T. P. (2009). Study of channel angle influence on material flow and strain inhomogeneity in equal channel angular pressing using 3D finite element simulation. *Journal of Materials Processing Technology, 209*(1), 89-95.

Dixit, P. M., & Dixit, U. S. (2008). *Modeling of metal forming and machining processes: by finite element and soft computing methods*: Springer.

El Mehtedi, M., Forcellese, A., Mancia, T., Simoncini, M., & Spigarelli, S. (2019). A new sustainable direct solid state recycling of AA1090 aluminum alloy chips by means of friction stir back extrusion process. *Procedia CIRP, 79*, 638-643.

Faraji, G., Kim, H. S., & Kashi, H. T. (2018). *Severe plastic deformation: methods, processing and properties*: Elsevier.

Faraji, G., Taherkhani, E., & Sabour, M. R. (2024). Cyclic severe plastic deformation processes.

Jafarlou, D., Zalnezhad, E., Hassan, M., Ezazi, M., Mardi, N., Hamouda, A., Yoon, G. H. (2016). Severe plastic deformation of tubular AA 6061 via equal channel angular pressing. *Materials & Design*, 90, 1124-1135.

Lee, D. J., & Kim, H. S. (2014). Finite element analysis for the geometry effect on strain inhomogeneity during high-pressure torsion. *Journal of Materials Science*, 49(19), 6620-6628.

Li, Y., Ng, H. P., Jung, H.-D., Kim, H.-E., & Estrin, Y. (2014). Enhancement of mechanical properties of grade 4 titanium by equal channel angular pressing with billet encapsulation. *Materials Letters,* 114, 144-147.

Lowe, T. C., & Valiev, R. Z. (2000). Investigations and applications of severe plastic deformation (Vol. 80): Springer Science & Business Media.

Majidabad, M. A., Eftekhari, M., & Faraji, G. (2023). Characterization of Mg–9Al–1Zn-0.2 Mn alloy tubes processed by a new modified tube cyclic expansion extrusion (M-TCEE) process. *Journal of Materials Research and Technology*, 24, 7989-8001.

Manafi, B., Shatermashhadi, V., Abrinia, K., Faraji, G., & Sanei, M. (2016). Development of a novel bulk plastic deformation method: hydrostatic backward extrusion. *The International Journal of Advanced Manufacturing Technology*, 82(9), 1823-1830.

Mao, Q., Zhang, Y., Guo, Y., & Zhao, Y. (2021). Enhanced electrical conductivity and mechanical properties in thermally stable fine-grained copper wire. *Communications Materials*, 2(1), 46.

Motallebi Savarabadi, M., Faraji, G., & Eftekhari, M. (2021). Microstructure and mechanical properties of the commercially pure copper tube after processing by hydrostatic tube cyclic expansion extrusion (HTCEE). *Metals and Materials International*, 27(6), 1686-1700.

Rahimi, F., Eivani, A., & Kiani, M. (2015). Effect of die design parameters on the deformation behavior in pure shear extrusion. *Materials & Design,* 83, 144-153.

Rahimi, H., Taherkhani, E., Sabour, M., & Faraji, G. (2025). Fabrication of Cu–Al MMC with randomly-oriented continuous intermetallic layers via entangled twisting fiber plasma sintering. *Journal of Materials Research and Technology.*

Shatermashhadi, V., Manafi, B., Abrinia, K., Faraji, G., & Sanei, M. (2014). Development of a novel method for the backward extrusion. *Materials & Design (1980-2015)*, 62, 361-366. doi:https://doi.org/10.1016/j.matdes.2014.05.022

Taherkhani, E., Sabour, M., Esmaeilnia, A., Aghchai, A. J., Straumal, B., & Faraji, G. (2025). Refinement of ultrahigh aspect ratio pure aluminum through novel hydrostatic twist extrusion: microstructural and mechanical insights. *Journal of Materials Research and Technology*.

Taherkhani, E., Sabour, M., & Faraji, G. (2024). Sustainable magnesium recycling: Insights into grain refinement through plastic deformation-assisted solid-state recycling (SSR). *Journal of Magnesium and Alloys, 12*(10), 3947-3966.

Taherkhani, E., Sabour, M., Khajepour, M., Safahi, H., Aghchai, A. J., Baniasadi, M., & Faraji, G. (2025). Hydrostatic twist extrusion: the effects of hydrostatic fluid pressure on deformation characteristics. *International Journal on Interactive Design and Manufacturing (IJIDeM)*, 1-12.

Toth, L. S., Chen, C., Pougis, A., Arzaghi, M., Fundenberger, J.-J., Massion, R., & Suwas, S. (2019). High pressure tube twisting for producing ultra fine grained materials: a review. *Materials Transactions, 60*(7), 1177-1191.

Uyyuru, R. K., & Valberg, H. (2006). Physical and numerical analysis of the metal flow over the punch head in backward cup extrusion of aluminium. *Journal of Materials Processing Technology, 172*(2), 312-318.

Valiev, R. Z., Estrin, Y., Horita, Z., Langdon, T. G., Zehetbauer, M. J., & Zhu, Y. (2016). Producing bulk ultrafine-grained materials by severe plastic deformation: ten years later. *JOM, 68*(4), 1216-1226.

Wang, J. T., Li, Z., Wang, J., & Langdon, T. G. (2012). Principles of severe plastic deformation using tube high-pressure shearing. *Scripta Materialia, 67*(10), 810-813.

Zeng, J., Li, J., Dong, S., Wang, F., Wang, F., Jin, L., & Dong, J. (2024). Optimization of hot backward extrusion process parameters for seamless tube of Mg-8Gd-3Y alloy by finite element simulation. *Journal of Materials Engineering and Performance, 33*(5), 2453-2461.

Zohrevand, M., Rezaei, A. R., Sabour, M. R., Taherkhani, E., & Faraji, G. (2023). Recent progress on SPD processes empowered by hydrostatic pressure. *Materials Transactions, 64*(8), 1663-1672.